

Supplementary Information

All reagents and solvents are commercially available and were used without further purification. Acetonitrile was dried with a molecular sieve (4 Å).

MOF syntheses were carried out according to Farha *et al.* [16] In a typical experiment 10 mg, 0.049 mmol of the precursor $\text{Pd}(\text{NO}_3)_2 \cdot 2\text{H}_2\text{O}$ and 7 cm³ of the dried acetonitrile were added to *ca.* 100 mg of the activated MOF (*in-vacuo* at 130 °C, overnight) in a 1:10 Pd:Zr ratio, and heated gently heated and stirred (50°C, 24 hours). After filtration, the solid product was washed with dried acetonitrile, dried and stored under an inert Ar atmosphere. The reduction of the Pd precursor was carried out in hydrogen stream (10 dm³ hour⁻¹, 1.3 bar overpressure, 6 hours, at 210 °C), using a custom-made cell in a tube furnace.

High Angle Annular Dark Field-Scanning Transmission Electron Microscopy (HAADF-STEM) micrographs have been obtained (Figure 2) using an FEI Titan G2 TEM/STEM operating at 200kV with a probe size of ~0.2 nm and probe current of ~0.25 nA.

X-ray photoelectron spectroscopy (XPS) was carried out using a Kratos AXIS Ultra DLD instrument. The X-ray source was monochromated Al K-alpha (1486.7 eV) and a pass energy of 40 eV was used leading to a resolution better than 0.15 eV. A filament coaxial to the analyser was used as an electron source for charge neutralisation and the data were calibrated to a C 1s main peak at 284.8 eV. Data were analysed in CasaXPS using Shirley backgrounds [19] and Gaussian-Lorentzian line shapes.

Synchrotron X-ray experiments were conducted at Japan Atomic Energy Agency (JAEA) beam line of BL22XU [20] at SPring-8. Powder samples were loaded in kapton capillaries with a diameter of 1.0 mm. Data were collected at room temperature using an amorphous silicon area detector manufactured by Perkin Elmer. The detector was mounted orthogonal to the incident X-ray beam of 70.2054 keV ($\lambda=0.176602$ Å). The sample-to-detector distance was 730 mm.

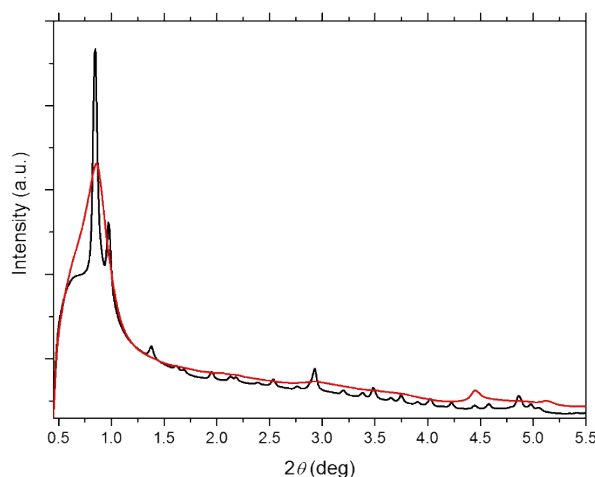


Figure S1 Synchrotron X-ray Powder Diffractogram of $\text{NH}_2\text{-UiO-66}$ (black) and Pd supported on $\text{NH}_2\text{-UiO-66}$ (red)

From the comparison of PXRD patterns of the $\text{NH}_2\text{-UiO-66}$ and the Pd-supported $\text{NH}_2\text{-UiO-66}$ (Figure S1), it is apparent that the diffraction peak intensity of $\text{NH}_2\text{-UiO-66}$ are substantially reduced upon the addition of Pd. It should however be mentioned that this is a consequence of pore filling by Pd rather than amorphisation of the MOF lattice as highlighted by the strong lattice fringing observed in the TEM micrographs of the Pd-supporting $\text{NH}_2\text{-UiO-66}$ (Figure S2).

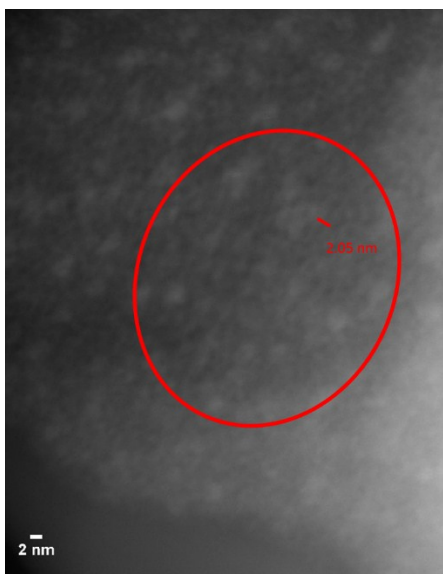


Figure 2 HAADF STEM micrograph of $\text{NH}_2\text{-UiO-66}$ supporting Pd nanoclusters highlighting strong lattice fringing of the MOF matrix

The lattice parameter observed in the TEM micrograph, 2.05 nm, is in good agreement with that determined for UiO-66 [10], which is isostructural to $\text{NH}_2\text{-UiO-66}$. This highlights that retention of the MOF's crystallinity upon Pd embedding.

¹⁹ D.A. Shirley, *Phys. Rev. B Condens. Matter*, 1972, **5**, 4709-4713

²⁰ T. Watanuki, A. Machida, T. Ikeda, A. Ohmura, H. Kaneko, K. Aoki, T. Sato and A. P. Tsai, *Philos. Mag.* 2007, **87**, 2905-2911.